FINAL PROJECT REPORT # 00042134-05-3A

GRANT: DTRT13-G-UTC45
Project Period: 6/1/2014 – 12/31/2019

Volume IV:

Performance of Fiber-Reinforced Self-Consolidating Concrete for Repair of Bridge Sub-Structures and Fiber Reinforced Super Workable Concrete for Infrastructure Construction

Participating Consortium Member:

University of Oklahoma, Norman, Oklahoma

Authors:
Jeffery S. Volz, SE, PE, PhD (Principal Investigator)
Jonathan T. Drury, PhD
Jacob G. Choate
Corey M. Wirkman

RE-CAST:
REsearch on Concrete Applications for Sustainable Transportation
Tier 1 University Transportation Center

MISSOURI S&T
MIAMI
SOUTHERN UNIVERSITY AND A&M COLLEGE
RUTGERS

DISCLAIMER

The contents of this report reflect the views of the authors, who are responsible for the facts and the accuracy of the information presented herein. This document is disseminated under the sponsorship of the U.S. Department of Transportation's University Transportation Centers Program, in the interest of information exchange. The U.S. Government assumes no liability for the contents or use thereof.

TECHNICAL REPORT DOCUMENTATION PAGE

1. Report No. RECAST UTC # 00042134-05-3A	**2. Government Accession No.**	**3. Recipient's Catalog No.**
4. Title and Subtitle Volume IV: Performance of Fiber-Reinforced Self-Consolidating Concrete for Repair of Bridge Sub-Structures and Fiber-Reinforced Super Workable Concrete for Infrastructure Construction		**5. Report Date** January 2020 **6. Performing Organization Code:**
7. Author(s) Jeffery S. Volz, Jonathan T. Drury, Jacob G. Choate, Corey M. Wirkman		**8. Performing Organization Report No.** Project # 00042134-05-3A
9. Performing Organization Name and Address RE-CAST – Missouri University of Science and Technology 500 W. 16th St., 223 ERL Rolla, MO 65409-0710		**10. Work Unit No.** **11. Contract or Grant No.** USDOT: DTRT13-G-UTC45
12. Sponsoring Agency Name and Address Office of the Assistant Secretary for Research and Technology U.S. Department of Transportation 1200 New Jersey Avenue, SE Washington, DC 20590		**13. Type of Report and Period Covered:** Final Report Period: 6/1/2014 – 12/31/2019 **14. Sponsoring Agency Code:**
15. Supplementary Notes The investigation was conducted in cooperation with the U. S. Department of Transportation.		
16. Abstract The main objectives of this research project were to: • Develop mix designs and examine the fresh and hardened properties of SCC and FR-SCC using locally-available materials, steel and synthetic macro-fibers, and varying per-centages of a Type-K shrinkage-compensating cement. • Investigate compatibility and bond strength of FR-SCC as a repair material and select mixes that yield the best performance for the subsequent phase of the research project, namely full-scale testing. • Evaluate the structural performance of full-scale repaired beams using the FR-SCC mixes developed previously. • Transition the technology from the laboratory to the field with an implementation project involving the repair of in-service bridge girders followed by removal and testing of the girders to failure.		
17. Key Words Bridge substructures; Bridge superstructures; Fiber reinforced concrete; Infrastructure; Maintenance; Performance based specifications; Self describing data. Crack resistance, Expansive agent, Fiber reinforced concrete, Flexural behavior, Macro fibers, Micro fibers, Repair, Super workable concrete.	**18. Distribution Statement** No restrictions. This document is available to the public.	
19. Security Classification (of this report) Unclassified	**20. Security Classification (of this page)** Unclassified	**21. No of Pages** 49

Form DOT F 1700.7 (8-72) Reproduction of form and completed page is authorized.

FINAL Report

Performance of Fiber-Reinforced Self-Consolidating Concrete for Repair of Bridge Sub-Structures and Fiber-Reinforced Super-Workable Concrete for Infrastructure Construction

By

Jeffery S. Volz, SE, PE, PhD (Principal Investigator)
Jonathan T. Drury, PhD
Jacob G. Choate
Corey M. Wirkman

University of Oklahoma, Norman, Oklahoma

TABLE OF CONTENTS

Page

TABLE OF CONTENTS (cont'd)

LIST OF ILLUSTRATIONS

Page

LIST OF ILLUSTRATIONS (cont'd)

Page

LIST OF TABLES

Page

1 INTRODUCTION

1.1 Problem Statement, Background, and Justification

Deterioration and damage of reinforced concrete elements accounts for significant annual expenditures by state and federal transportation agencies on bridge maintenance, repair, or replacement. While new bridges are designed to function for 75 to 100 years, they will still require substantially more long-term attention and service support. Because of the limited infrastructure budget, an increased service life is also being expected out of infrastructure repair sections. In the coming years, maintenance and construction costs associated with infrastructure throughout the country will continue to increase faster than available matching funds. A recent survey by the United States Department of Transportation classified roughly 27.5 percent of the nearly 600,000 bridges with spans over 20 feet as "structurally deficient" and noted that "preservation strategies will become paramount" as funding continues to shrink (USDOT, 2014). According to the Turner Fairbank Highway Research Center, there is about 2.3 billion square feet of bridge-deck surface associated with the federal highway system. For each year that the lifetime of a bridge is extended, approximately $8 per square foot will be saved (Kassimi et al., 2014).

The rising costs of materials and labor, as well as the demand for faster construction, has prompted development of cheaper, faster alternatives to conventional building techniques. Self-consolidating concrete (SCC) is a high-performance concrete characterized by its ability to flow without segregation under its own weight. In addition, eliminating vibration cuts down on the labor needed and speeds up construction. This increase in speed results in faster placement rates, cost savings, and fewer traffic disruptions. The reduction of equipment usage also lessens wear and tear and noise levels in both concrete plants and at construction sites, improving jobsite safety. Furthermore, lack of vibration reduces aggregate segregation, honeycombing, and voids in the concrete. In repair applications, SCC has proved to be advantageous in facilitating the repair operations, including hard-to-reach areas and congested sections. Many of these applications can be found in bridge substructures (e.g., piers, girders, pile caps, abutments).

The first documented case study involving the use of SCC in repair operations involved the rehabilitation of a parking garage in downtown Sherbrooke, Quebec, in 1996. SCC was used for the repair of the bottom and vertical sides of a 20-foot-long beam exhibiting advanced corrosion damage situated under an expansion joint at the entrance to the parking structure. The repair section contained longitudinal reinforcing bars and stirrups anchored into the existing concrete that presented serious obstacles for the spread of fresh concrete. The concrete was cast from two 4-inch diameter holes drilled from the upper deck of the beam along the outer length of the beam between the existing concrete and formwork. The developed SCC mix was shown to flow under its own weight along the highly restricted section and around the vertical side to fill the opposite side of the formwork through narrow spacing. Due to its success, the Quebec Department of Transportation developed its first performance-based specifications for SCC in 1997 and has used SCC in several infrastructure rehabilitation projects. Experience with SCC has shown that in addition to its ease of casting characteristics, the concrete can exhibit high durability and good bond to existing surfaces and reinforcement (Kassimi et al., 2014).

Successful experience with the performance of SCC as a superior repair material has attracted the attention of construction firms and departments of transportation. Examples of the repair of damaged bridge substructures are shown in Figures 1.1 thru 1.3.

Figure 1.1: SCC Used in the Repair of Bridge Pier Caps (Khayat et al., 2010)

Figure 1.2: SCC Used in the Repair of Bridge Piles (Ozyildirim, 2013)

Figure 1.3: SCC Used in the Repair of Bridge Columns and Pier Caps (Ozyildirim, 2013)

As in other repair applications, repair sections constructed with concrete are prone to cracking due to restrained shrinkage. Recently, fiber reinforcement has been used in SCC to control cracking and increase tensile and flexural strength. Fiber reinforced self-consolidating concrete (FR-SCC) combines the benefits of SCC in the fresh state with improved performance in the hardened state. One of the earliest uses of FR-SCC was in the Jarry/Querbes Underpass in Montreal. The structure

had undergone severe degradation due to aggressive exposure to frost action. The project was successfully repaired with the use of FR-SCC. The use of synthetic structural fibers was beneficial in obtaining only small and finely distributed surface cracking. This project is shown in Figure 1.4.

Figure 1.4: FR-SCC Used in the Repair of the Jarry/Querbes Underpass (Khayat et al., 2005)

The performance of FR-SCC depends on the type of fibers in use. Several fiber types exist on the market, and they should be selected wisely to secure the intended objectives. Kassimi and Khayat carried out an extensive investigation to evaluate the performance of various fibers in SCC targeted for repair applications (Kassimi et al., 2014). The concrete mixtures were tested for workability, mechanical properties, drying and restrained shrinkage, flexural creep, and some structural behavior in flexure. Polypropylene fibers, a hybrid of steel and polypropylene, and steel fibers were used. Although limited in scope, the investigation revealed that the incorporation of fibers along with an expansive agent (EA) can enhance the resistance to restrained shrinkage. The improvement was greater than that observed in FR-SCC without EA or that for SCC with EA. In addition, a synergistic effect was observed where the presence of fibers and EA secured superior resistance to cracking in concrete. This is a key requirement to enhance the service life of a repair.

1.2 Research Objectives

The main objectives of this research project were to:

- Develop mix designs and examine the fresh and hardened properties of SCC and FR-SCC using locally-available materials, steel and synthetic macro-fibers, and varying percentages of a Type-K shrinkage-compensating cement.

- Investigate compatibility and bond strength of FR-SCC as a repair material and select mixes that yield the best performance for the subsequent phase of the research project, namely full-scale testing.

- Evaluate the structural performance of full-scale repaired beams using the FR-SCC mixes developed previously.

- Transition the technology from the laboratory to the field with an implementation project involving the repair of in-service bridge girders followed by removal and testing of the girders to failure.

2 CONCRETE MATERIALS, PROPORTIONS, AND TESTING

The following chapter discusses the materials used to develop the control, SCC, and FR-SCC mix designs. The materials used for this research study included cementitious materials, fine and coarse aggregates, concrete admixtures, synthetic fibers, and reinforcing steel.

2.1 Cementitious Materials

After consulting with the Oklahoma Department of Transportation (ODOT), the cementitious materials chosen for this study consisted of Type I cement, Class C fly ash, and Type K shrinkage-compensating cement. Class C fly ash is the predominant fly ash available in the State of Oklahoma, and Type K shrinkage-compensating cement is the only shrinkage compensating material currently allowed in the ODOT Specifications. Type K cement is an expansive cement containing anhydrous calcium alumniosulfate, calcium sulfate, and uncombined calcium oxide. The chemical and physical properties of these cementitious materials are shown in Table 2.1.

Table 2.1: Chemical and Physical Properties of Cementitious Materials

Property	Type I Cement	Class C Fly Ash	Type K Cement
SiO_2, %	19.8	35.5	7.7
Al_2O_3, %	4.8	20.5	7.0
Fe_2O_3, %	3.1	6.8	1.2
CaO, %	63.2	26.3	50.1
MgO, %	1.4	5.5	0.1
SO_3, %	3.1	2.4	26.0
Na_2O eq., %	-	-	0.6
LOI, %	2.7	0.3	2.3
Specific Gravity	3.1	2.7	3.0
Blaine Fineness, m^2/kg	395	475	505

2.2 Aggregates

Aggregates for the research study consisted of natural river sand and limestone donated by Dolese Bros. Co. from their Davis Quarry, Figure 2.1, and river gravel donated by Metro Materials, Norman, Oklahoma. The fine aggregate consisted of natural river sand while the coarse aggregates consisted of a No. 57 limestone gradation and a No. 7 river gravel gradation, shown in Figure 2.2. The aggregate gradations and ODOT gradation limits are provided in Tables 2.2, 2.3, and 2.4 for the sand, No. 57 limestone, and No. 7 river gravel, respectively, all of which met the requirements. The specific gravity, dry rodded unit weight (DRUW), absorption, and LA abrasion values for

each aggregate type are provided in Table 2.5. The No. 57 limestone and No. 7 river gravel coarse aggregates met the minimum abrasion resistance requirements of the ODOT specifications.

Figure 2.1: Dolese Bros. Co. Davis Quarry

Figure 2.2: #57 Limestone (l) and #7 River Gravel (r) Coarse Aggregates

2.3 Admixtures

The concrete mixtures developed in this study used two types of chemical admixtures to achieve the necessary durability and workability requirements. The first consisted of a synthetic-based air-entraining admixture (AEA) that met the requirements of ASTM C 260. The second consisted of a polycarboxylate-based water reducer/high range water reducer. This admixture met the requirements of ASTM C 494 for both a Type A water reducing admixture (WRA) and a Type F high range water reducing admixture (HRWRA). The dosages of both chemical admixtures were adjusted to achieve the desired air entrainment and flowability for each specific concrete mixture.

Table 2.2: Fine Aggregate Gradation and Percent Passing Limits

Sieve Size/No.	Sieve Opening (mm)	ODOT Lower Bound	Percent Passing Tested	ODOT Upper Bound
3/8”	9.5	100	100	100
#4	4.75	95	99	100
#8	2.36	80	95	100
#16	1.18	50	80	85
#30	0.60	25	47	60
#50	0.30	5	14	30
#100	0.15	0	2	10
#200	0.075	0	0	3

Table 2.3: No. 57 Limestone Coarse Aggregate Gradation and Percent Passing Limits

Sieve Size/No.	Sieve Opening (mm)	ODOT Lower Bound	Percent Passing Tested	ODOT Upper Bound
1-1/2”	37.5	100	100	100
1”	25	95	99	100
3/4"	19	-	79	-
1/2"	12.5	25	47	60
3/8”	9.5	-	10	-
#4	4.75	0	1	10
#8	2.36	0	0.5	5
#16	1.18	-	0.4	-
#200	0.075	0	0.04	2

Table 2.4: No. 7 River Gravel Aggregate Gradation and Percent Passing Limits

Sieve Size/No.	Sieve Opening (mm)	ODOT Lower Bound	Percent Passing Tested	ODOT Upper Bound
3/4"	19.0	100	100	100
1/2”	12.5	90	95	100
3/8”	9.5	40	70	70
#4	4.75	0	13	15
#8	2.36	0	4	5
#16	1.18	-	3	-

Table 2.5: Aggregate Properties

Aggregate	Specific Gravity	DRUW (pcf)	Absorption (%)	LA Abrasion (%)
Sand	2.58	-	0.40	-
No. 57	2.64	101.5	0.86	24
No. 7	2.83	105.4	0.72	20

2.4 Fibers

The concrete mixtures developed in this study used both steel and synthetic macro-fibers. The two fibers were chosen due to their similar physical dimensions yet recognizing that steel fibers are considerably stronger than synthetic fibers. The steel fibers were a high ductility, very high tensile strength, hooked wire fiber manufactured by Bekaert, marketed under the trade name Dramix® 5D. These fibers were engineered for use as supplemental flexural and shear reinforcement as well as to control shrinkage and temperature cracking. The synthetic fibers were a high-tensile strength, high modulus of elasticity, embossed fiber manufactured from a blend of polypropylene resins by BASF, marketed under the trade name MasterFiber MAC Matrix®. These fibers were engineered for use as secondary reinforcement to control shrinkage and temperature cracking as well as settlement cracking. Material properties and the recommended dosages of the fibers are provided in Table 2.6. A photograph of the steel and synthetic fibers is shown in Figure 2.3.

Table 2.6: Steel and Synthetic Fiber Properties and Recommended Dosages

Property	Steel Fibers	Synthetic Fibers
Specific Gravity	7.83	0.91
Tensile Strength	320 ksi	85 ksi
Nominal Length	1.97 in.	2.10 in.
Nominal Aspect Ratio	68	70
Recommended Dosages (% volume)	0.25-1.0	0.25-0.75

2.5 Reinforcing Steel

In order to determine the yield stress, ultimate stress, and modulus of elasticity of the reinforcing steel used in the full-scale beam test specimens, tension tests were performed in accordance with ASTM E 8-09. The tests were performed on three specimens of each reinforcing bar size used in the full-scale beam tests, with each specimen measuring 36 in. in length. The results of the test are summarized in Table 2.7.

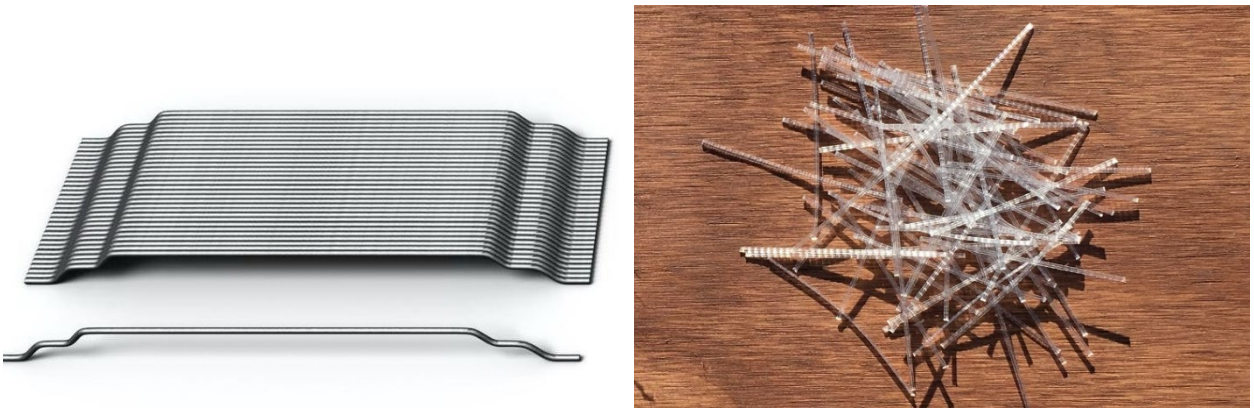

Figure 2.3: Steel (l) and Synthetic (r) Macro-Fibers

Table 2.7: Reinforcing Steel Tension Test Results

Bar Size	Yield Stress (ksi)	Ultimate Stress (ksi)	Modulus of Elasticity (ksi)
#3	72.9	101.5	28,651
#6	78.2	109.1	28,963
#7	79.7	111.3	28,625

2.6 Mixture Proportions

The purpose of this research project is to develop fiber-reinforced, self-consolidating concrete for repair of bridge superstructures and substructures. The baseline mixtures for comparison are two standard ODOT mixes, one for substructure construction, Class A, and one for bridge superstructure construction, Class AA. The ODOT requirements for these two standard mixes are shown in Table 2.8. The slump requirement is prior to the addition of any water reducer or high range water reducer.

Table 2.8: Baseline ODOT Mix Design Requirements

Class of Concrete	Minimum Cement Content (lb/yd^3)	Air Content (%)	Water/Cementitious Material Ratio	Slump (in)	Minimum 28-day Compressive Strength (psi)
A	517	6±1.5	0.25 – 0.48	2±1	3,000
AA	564	6.5±1.5	0.25 – 0.44	2±1	4,000

2.7 Test Methods

The test methods performed on the control, SCC, and FR-SCC concretes developed in this research project include fresh concrete properties, hardened concrete properties, small-scale bond performance, and full-scale structural performance. The standard fresh and hardened concrete property tests are summarized in Table 2.9. Details of the small-scale bond performance and full-scale structural performance testing are discussed in Chapters 4 and 5, respectively.

Table 2.9: Standard Fresh and Hardened Concrete Tests

Category	Test Property	ASTM Reference
Fresh	Slump	C 143
	Slump Flow	C 1611
	J-Ring Passing Ability	C1621
	Unit Weight	C 138
	Air Content	C 231
Hardened	Compressive Strength	C 39
	Modulus of Rupture	C 78
	Split Cylinder Strength	C 496
	Modulus of Elasticity	C 469

3 CONTROL, SCC, AND FR-SCC MIX DESIGN DEVELOPMENT

The following chapter discusses the control, SCC, and FR-SCC mix design development. The control concrete is based on the requirements for an ODOT Class AA mix. The SCC and FR-SCC mixes are based on work done at Missouri University of Science and Technology (Missouri S&T) and adjusted based on locally-available materials in the State of Oklahoma as well as recommendations from ODOT.

3.1 Control Mix Design Development

In developing the control mix design, the research team worked with ODOT and Dolese Bros. Dolese Bros. is a major aggregate and ready mix concrete supplier in Oklahoma, Kansas, and Texas who also donated a significant amount of materials to the project in terms of aggregate, cement, fly ash, fibers, and ready mixed concrete. After several trial mixes and consultation with ODOT, two final control mix designs were selected for further testing. The primary difference between the two mix designs is the water/cement ratio and the use of fly ash. The final mix designs are shown in Table 3.1, and the fresh and hardened properties are shown in Table 3.2.

Table 3.1: Class AA Mix Designs

Mix Design Components per Cubic Yard		
Material	Mix No. 1	Mix No. 2
Cement (Type I/II)	564 lb.	470 lb.
Fly Ash (Class C)	-	118 lb. (20% by mass)
w/cm	0.45	0.35
Fine Aggregate (River Sand)	1252 lb.	1323 lb.
Coarse Aggregate (#57 Limestone)	1676 lb.	1857 lb.
S/A by Volume	0.40	0.42
AEA	4.2 oz. (0.75 oz./cwt)	4.4 oz. (0.75 oz./cwt)
WRA	11.3 oz. (2.0 oz./cwt)	26.7 oz. (4.53 oz./cwt)

Based on the results and recommendations from both ODOT and Dolese, the decision was made to move forward with Mix No. 2 for the Class AA control mix.

Table 3.2: Class AA Fresh and Hardened Properties

Property	Mix No. 1	Mix No. 2
Slump Prior to Addition of Water Reducer	4 in.	1 in.
Slump After Addition of Water Reducer	8 in.	4 in.
Air Content	6.0%	7.0%
Temperature	71.5°F	70.0°F
7-Day Compressive Strength	3,610 psi	4,480 psi
28-Day Compressive Strength	5,130 psi	6,110 psi
Modulus of Rupture	462 psi	547 psi
Modulus of Elasticity	4,001,000 psi	4,203,000 psi

3.2 SCC Mix Design Development

In developing the SCC mix design, the research team sought to maximize the resistance of the repair material to shrinkage and thermally induced cracking. In application, the repair material will be cast against existing concrete, and as a result, differential shrinkage and thermal stresses often lead to cracking in these types of applications, which significantly increases the potential for future deterioration. To accomplish this trait, the SCC mix design was developed with the aim of maximizing the percentages of fly ash, Type K shrinkage-compensating cement, and fiber content. The fly ash will help reduce heat generation, thereby reducing the potential for thermally induced cracking. The Type K shrinkage-compensating cement will potentially result in a slightly expansive repair material, which will place the repair in compression instead of tension. While in the event that the fly ash and Type K cement do not eliminate the potential for shrinkage and thermally induced cracking, the macro-fibers will control the size of any resulting cracks, thereby reducing the potential for deterioration of the repair material. Based on these requirements, the initial specifications used to develop the SCC mix design are shown in Table 3.3.

After several trial batches, the team arrived at the initial SCC mix design shown in Table 3.4. Table 3.5 contains the fresh and hardened material properties, and Figure 3.1 shows the slump flow behavior. In the course of developing the SCC mix design, the research team found that the Type K shrinkage-compensating cement (Komponent) reduced segregation compared to trial mixes without the expansive agent. In many ways, the Komponent acted as a viscosity modifying admixture. However, the Komponent also reduced setting time and lead to a noticeable loss in slump flow over time, which is typical of a Type K expansive agent and was also found by the Missouri S&T research team. The slump flow decreased from 30.0 inches to 21 inches after only 10 minutes.

Table 3.3: Initial SCC Mix Design Specification

Characteristic	Value
Cementitious Content	750 lb/yd^3
Fly Ash Replacement (by mass)	30%
Type K Replacement (by mass)	15%
w/c Ratio	0.40
S/A by Volume	0.50
Target Slump Flow	28.0 in.
Minimum Compressive Strength	4,000 psi

Table 3.4: Initial SCC Mix Design

Components per Cubic Yard	
Material	Amount
Cement (Type I/II)	412.5 lb.
Fly Ash (Class C)	225 lb. (30% by mass)
Komponent (Type K Expansive Agent)	112.5 lb. (15% by mass)
w/cm	0.38
Fine Aggregate (River Sand)	1404 lb.
Coarse Aggregate (#7 River Gravel)	1261 lb.
S/A by Volume	0.50
AEA	8.25 oz. (1.1 oz./cwt)
HRWRA	52.5 oz. (7.0 oz./cwt)

Table 3.5: Initial SCC Fresh and Hardened Properties

Property	Value
Slump Prior to Addition of Water Reducer	4 in.
Slump Flow	29.5 in.
VSI	0
J-Ring	28.7
Air Content	6.4%
Temperature	72.5°F
7-Day Compressive Strength	4,370 psi
28-Day Compressive Strength	6,140 psi
Modulus of Rupture	633 psi
Modulus of Elasticity	4,570,000 psi

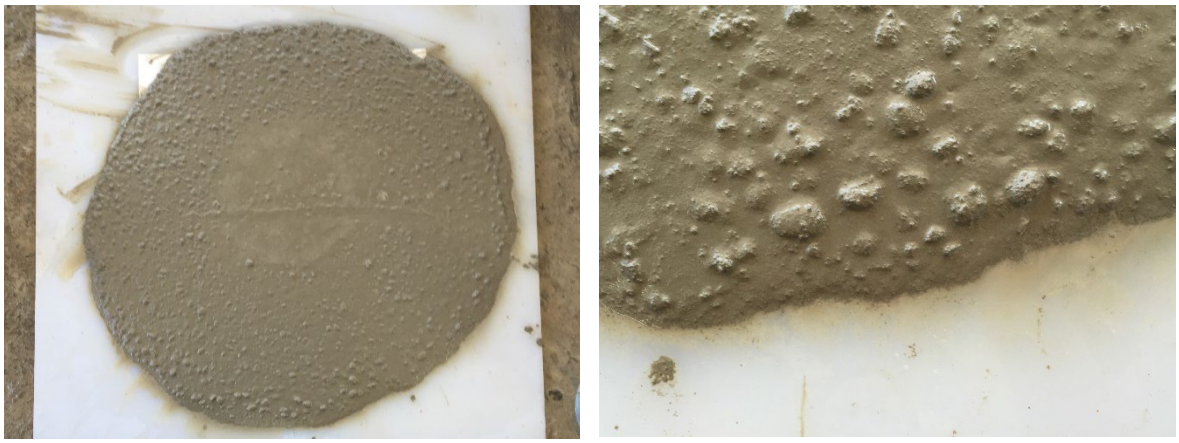

Figure 3.1: Initial SCC Mix Design Slump Flow Behavior, Overall Spread (l) and Edge View (r)

The research team consulted with the manufacturer of the Type K expansive agent, CTS Cement Manufacturing Corporation (CTS), on potential solutions to mitigate the slump flow loss. After several discussions and numerous trial batches, the final solution involved dosing the concrete with citric acid and continuing to mix between slump flow measurements. Citric acid is often used as a retarder for Komponent, which is a calcium sulfoaluminate (CSA) cement, and can be redosed multiple times without any decrease in concrete performance. After several trial studies, the citric acid dosage was set to 0.35% by mass of the Komponent to be redosed at intervals of 15 minutes. The results of the final slump flow loss study consisted of the following:

- Initial Slump Flow: 30.5 in. with a VSI of 0
- At 10 Minutes: 29.5 in. with a VSI of 0
- At 20 Minutes: 28.0 in. with a VSI of 0
- At 40 Minutes: 25.0 in. with a VSI of 0
- At 60 Minutes: 20.5 in. with a VSI of 0

3.3 FR-SCC Mix Design Development

In developing the FR-SCC mix designs, the research team examined both of the steel and synthetic macro-fibers discussed in Section 2.4. As mentioned previously, the two fibers were chosen due to their similar physical dimensions, both measuring approximately 2 inches in length, yet recognizing that steel fibers are considerably stronger than synthetic fibers. The fibers were added to the SCC mix developed previously at a 0.5% fiber volume dosage.

To maintain the desired slump flow of 28.0 inches, both FR-SCC mixes required an increase in the high range water reducing admixture (HRWRA). However, J-ring and L-box testing of the FR-SCC mixes revealed that the steel fibers required a higher dosage of HRWRA yet still experienced a noticeable decrease in passing ability. Furthermore, at the HRWRA dosages required to maintain flowability, the FR-SCC mix with the steel fibers suffered excessive settlement during the static column segregation test. Based on these results and discussions with both ODOT and Dolese, the decision was made to move forward with the synthetic fibers for further testing.

The research team continued to refine the FR-SCC mix design with the 0.5% synthetic fibers and citric acid retarder and developed a full-scale flow test to mimic the repair application. The setup for the full-scale flow test is shown in Figure 3.2 and uses the same formwork, access pipe, and funnel as that which will be used to construct the full-scale repaired beams. The FR-SCC successfully flowed the full 14-foot length of the formwork, with a depth of concrete at the placement point of 7 inches, and a depth of concrete at the far end of the formwork of 6-3/4 inches. The final FR-SCC mix designs are shown in Table 3.6 for both 10% Type K expansive agent and 15% Type K expansive agent. ODOT requested an evaluation of both Type K replacement percentages in order to provide more flexibility in future specifications.

Figure 3.2: Full-Scale Flow Test of FR-SCC Mix Design, 15% Type K Expansive Agent

Table 3.6: FR-SCC Mix Designs

Mix Design Components per Cubic Yard		
Material	10% Type K Mix	15% Type K Mix
Cement (Type I/II)	450 lb.	412.5 lb.
Fly Ash (Class C)	225 lb. (30% by mass)	225 lb. (30% by mass)
Komponent (Type K Expansive Agent)	75 lb. (10% by mass)	112.5 lb. (15% by mass)
w/cm	0.38	0.38
Fine Aggregate (River Sand)	1404 lb.	1404 lb.
Coarse Aggregate (#7 River Gravel)	1261 lb.	1261 lb.
S/A by Volume	0.50	0.50
Synthetic Fibers (MasterFiber MAC Matrix)	7.7 lb. (0.5% by vol.)	7.7 lb. (0.5% by vol.)
AEA	8.25 oz. (1.1 oz./cwt)	8.25 oz. (1.1 oz./cwt)
HRWRA	61.9 oz. (8.25 oz./cwt)	61.9 oz. (8.25 oz./cwt)
Citric Acid (Type K Retarder)	0.35% (by mass of Type K)	0.35% (by mass of Type K)

4 EVALUATION OF FR-SCC MATERIAL PROPERTIES, BOND, AND COMPATIBILITY

The following chapter contains an evaluation of the material properties, bond strength, and compatibility of the FR-SCC mix designs developed in the previous chapter. The FR-SCC mix designs were developed to maximize their resistance to shrinkage and thermally induced cracking as well as to facilitate their placement in congested and geometrically challenging applications.

4.1 Material Property Testing

The three mixes moving forward for further evaluation included the Class AA as the control as well as the two FR-SCC mixes, one with 10% Komponent replacement and the other with 15% Komponent replacement. The three mix designs are summarized in Table 4.1.

Table 4.1: Class AA (Control) and FR-SCC Mix Designs

Mix Design Components per Cubic Yard			
Material	Class AA	FR-SCC 10% Type K	FR-SCC 15% Type K
Cement (Type I/II)	470 lb.	450 lb.	412.5 lb.
Fly Ash (Class C)	118 lb. (20% by mass)	225 lb. (30% by mass)	225 lb. (30% by mass)
Komponent (Type K Expansive Agent)	-	75 lb. (10% by mass)	112.5 lb. (15% by mass)
w/cm	0.35	0.38	0.38
Fine Aggregate (River Sand)	1323 lb.	1404 lb.	1404 lb.
Coarse Aggregate (#57 Limestone)	1857 lb.	-	-
Coarse Aggregate (#7 River Gravel)	-	1261 lb.	1261 lb.
S/A by Volume	0.42	0.50	0.50
Synthetic Fibers (MasterFiber MAC Matrix)	-	7.7 lb. (0.5% by vol.)	7.7 lb. (0.5% by vol.)
AEA	4.4 oz. (0.75 oz./cwt)	8.25 oz. (1.1 oz./cwt)	8.25 oz. (1.1 oz./cwt)
HRWRA	26.7 oz. (4.53 oz./cwt)	61.9 oz. (8.25 oz./cwt)	61.9 oz. (8.25 oz./cwt)
Citric Acid (Type K Retarder)	-	0.35% (by mass of Type K)	0.35% (by mass of Type K)

Each of the three mixes underwent standard concrete material property testing, which included compressive strength, modulus of rupture, splitting tensile strength, and modulus of elasticity at 28 days of age. The results are shown in Table 4.2, which also includes the normalized mechanical properties of the three mixes. The modulus of rupture and modulus of elasticity were normalized with respect to square root of the compressive strength, while the split cylinder strength was normalized with respect to the compressive strength taken to the two-thirds power. These are common normalization techniques used to compare concretes with different compressive strengths.

Table 4.2: Class AA and FR-SCC Material Properties

Property	Class AA	FR-SCC 10% Type K	FR-SCC 15% Type K
Compressive Strength	5740 psi	5890 psi	6010 psi
Modulus of Rupture (MOR)	560 psi	621 psi	613 psi
Split Tensile Strength (TSP)	385 psi	532 psi	500 psi
Modulus of Elasticity (MOE)	4,038,000 psi	4,593,000 psi	4,534,000 psi
Normalized MOR	7.39	8.09	7.89
Normalized TSP	1.20	1.63	1.51
Normalized MOE	53,299	59,846	58,485

In terms of comparative performance, both FR-SCC mixes slightly outperformed the Class AA mix in terms of compressive strength. However, both FR-SCC mixes noticeably outperformed the Class AA mix in terms of normalized modulus of rupture and normalized split tensile strength, most likely due to the addition of the synthetic fibers, although the fibers would also add even more to the post-cracking strength of the concrete. The FR-SCC mixes also outperformed the Class AA mix in terms of stiffness, with higher normalized moduli of elasticity, most likely due to the stiffer river gravel coarse aggregate in the FR-SCC mixes compared to the softer limestone coarse aggregate in the Class AA mix.

4.2 Bond and Compatibility Testing

One of the most critical properties for a repair material is its ability to successfully bond with the substrate concrete. Higher bond strengths will usually translate into more effective repairs, both in terms of strength and durability. To evaluate bond and compatibility of the FR-SCC mixes with potential substrate concrete, the research team completed composite prism, slant shear, and direct pull-off tests of the three mix designs. For all three tests, the substrate material consisted of the Class AA concrete.

The composite prism and slant shear tests used standard modulus of rupture and compressive strength specimens, respectively, with a combination of substrate concrete and repair material. The composite prism test is based on a standard modulus of rupture prism with the top 3 inches consisting of the Class AA mix and the bottom 3 inches consisting of the FR-SCC mixes. The slant shear test is based on a standard 6x12 compressive strength cylinder with the substrate cast first

with the molds placed at a 30° angle to the horizontal and then the FR-SCC cast with the cylinder in a vertical orientation. The result is a joint between the two concretes at an angle of 30° to the vertical. The substrate concrete for both specimens is cast first and allowed to cure for 28 days prior to placement of the FR-SCC repair materials. Representative test specimen types are shown in Figure 4.1, where the darker concrete indicates the FR-SCC repair materials.

Figure 4.1: Composite Prism Test Specimen (l) and Slant Shear Test Specimen (r)

The direct pull-off test uses a 12 inch by 12 inch substrate base to which an overlay is placed of the material to be tested. Both layers are 2 inches thick, with the substrate placed and allowed to cure a minimum of 28 days prior to placing the overlay material. After sufficient curing of the overlay material, the overlay is cored to a depth of approximately 1/2-inch into the substrate, aluminum plugs are glued to the overlay, and the pull-off tester is attached to the plugs. Three pull-off tension tests are performed for each specimen, with the average pull-off strength characterizing the bond of the overlay with the substrate. It is preferable that the specimen fail within the substrate for maximum bond with the overlay. The pull-off test setup and a representative specimen are shown in Figure 4.2.

Figure 4.2: Pull-off Test Setup (l) and Pull-off Test Specimen (r)

Table 4.3 summarizes the results of the composite modulus of rupture, slant shear, and pull-off tests. The FR-SCC noticeably outperformed the Class AA for all three bond test measures, with the two FR-SCC mixes performing nearly identical. This higher bond performance is most likely due to the increased flowability of the FR-SCC mixes, which allows the material to penetrate deeper into the substrate, improving the mechanical portion of the bond strength. All composite MOR specimens failed by flexural cracking, identical to a standard MOR specimen, indicating sufficient bond for all three mixes. The slant shear specimens failed primarily in compression with some slight failures along the bond line. The majority of pull-off specimens failed either within the substrate or within the overlay, indicating maximum bond strength between the overlay and substrate material.

Table 4.3: Class AA and FR-SCC Bond Properties

Property	Class AA	FR-SCC 10% Type K	FR-SCC 15% Type K
Compressive Strength	5740 psi	5890 psi	6010 psi
Composite MOR	575 psi	646 psi	680 psi
Slant Shear	455 psi	589 psi	570 psi
Pull-off	301 psi	377 psi	411 psi

5 FULL-SCALE SPECIMEN DESIGN, FABRICATION, TESTING, AND EVALUATION

The following chapter discusses the design, fabrication, testing, and evaluation of full-scale beam specimens constructed with the mix designs developed previously. There were a total of nine full-scale beam specimens. Three specimens constructed with the Class AA mix design to serve as control specimens, and three repaired beams for each of the two FR-SCC mixes. The repaired beams mimic a field application of the FR-SCC concept and consist of an upper portion of Class AA concrete and a lower portion of FR-SCC material placed through access ports in the Class AA concrete after the Class AA mix reached at least 28 days of age.

5.1 Design and Fabrication of Full-Scale Control Beam Specimens

The design and fabrication of the control beam specimens was based on previous research on FR-SCC flexural repairs by Kassimi, et al. (2014). The beams used in this current study were 14 feet long with a cross-section of 12 inches by 18 inches. The longitudinal reinforcement consisted of four #6, ASTM A615, Grade 60, steel reinforcing bars. Transverse reinforcement against shear failure consisted of #3, ASTM A615, Grade 60, U-shaped stirrups. To ensure that a shear failure would not occur prior to a flexural failure, a stirrup spacing slightly less than the ACI 314-14 (2014) maximum stirrup spacing of one half of the effective depth was used throughout the span length. Two #4, ASTM A615, Grade 60, steel reinforcing bars were used along the top of the beams to anchor the stirrups and stabilize the reinforcing cages. Figures 5.1 and 5.2 detail the cross-sectional and elevation views of the control beam specimens, respectively.

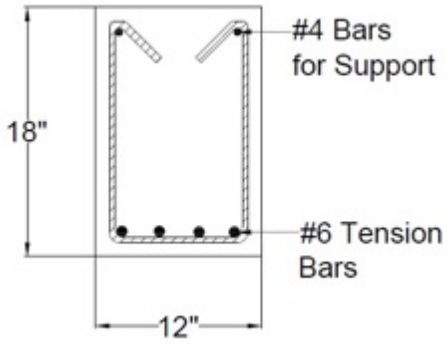

Figure 5.1: Full-Scale Control Beam Specimen Cross-Section

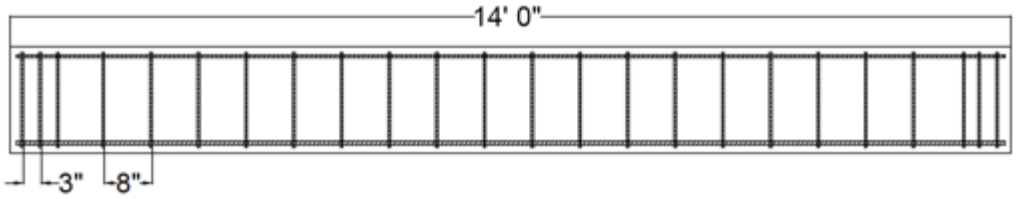

Figure 5.2: Full-Scale Control Beam Specimen Elevation

Once the reinforcing cage construction was complete, strain gages were installed on two of the longitudinal reinforcing bars near midspan, as shown in Figure 5.3. The strain gages were installed to verify that a flexural failure occurred. After grinding and cleaning of the reinforcing steel, each gage was attached using cyanoacrylate adhesive and then wrapped in a butyl rubber tape and aluminum foil for protection during the concrete placement. The lead wires for the strain gages were fed to the top of each cage and secured to the reinforcing steel with plastic zip ties. A data acquisition system monitored the strains in the reinforcing steel during the load test.

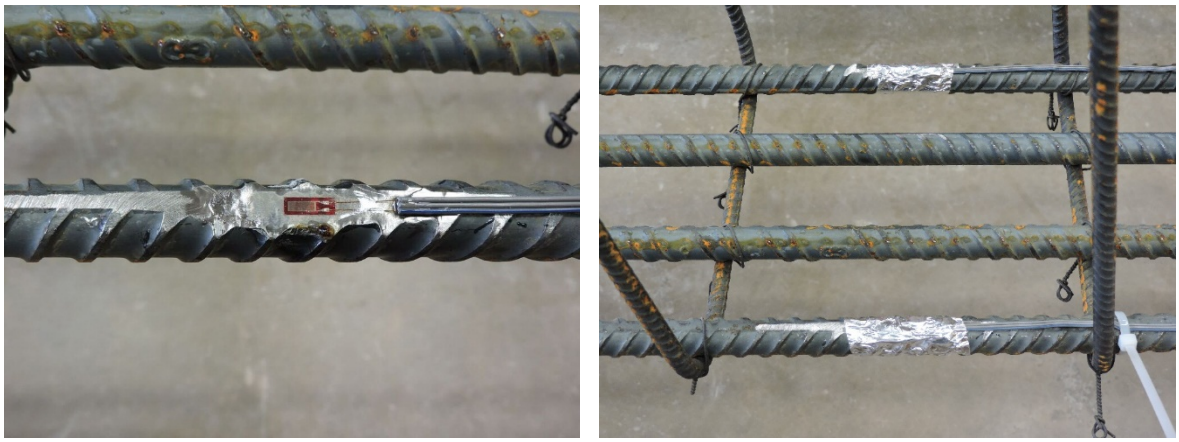

Figure 5.3: Strain Gages Installed Near Midspan of Longitudinal Reinforcing Steel

The Class AA mix was delivered by Dolese Bros. and placed into the beam forms using a concrete bucket, as shown in Figure 5.4. The beams were filled in two layers. After the first layer was poured, the concrete was vibrated to reduce air pockets and ensure proper consolidation. Once the last layer was poured and vibrated, the top was screeded and smoothed with finishing trowels, as shown in Figure 5.4. During the finishing process, premade steel hooks were vibrated into the top of the beams for transporting the specimens. The beams and companion small scale specimens were moist cured for 7 days.

Figure 5.4: Full-Scale Control Beam Specimen Concrete Placement (l) and Finishing (r)

5.2 Design and Fabrication of Full-Scale FR-SCC Repaired Beam Specimens

The design and fabrication of the FR-SCC repaired beam specimens was based on previous research on FR-SCC flexural repairs by Kassimi, et al. (2014). The beam specimens were identical to the control specimens except that the concrete was cast in two separate placements, with a repair zone along the bottom of the beams with an average depth of 6 inches. This depth was chosen to represent the effective tension zone of the beam, which must often be repaired given advanced corrosion of the bottom reinforcing steel within an actual structure. The depth was slightly sloped from 7 inches at one end of the beam to 5 inches at the other end to assist with the flow of the FR-SCC, which was placed from the end of the member with the 7-inch-thick void depth. Figures 5.5 and 5.6 detail the cross-sectional and elevation views of the FR-SCC repaired beam specimens, respectively.

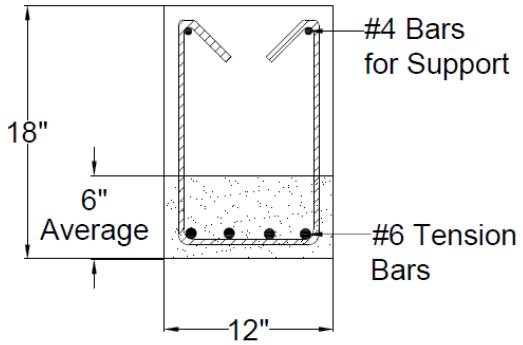

Figure 5.5: Full-Scale FR-SCC Repaired Beam Specimen Cross-Section

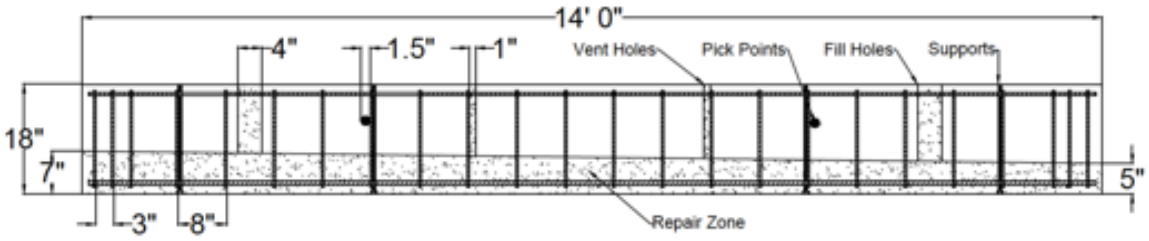

Figure 5.6: Full-Scale FR-SCC Repaired Beam Specimen Elevation

In order to simulate a true repair of the flexural zone, the control concrete was cast first and then flipped so that the repair concrete would be cast along the bottom. In order to accomplish this step, two vertical 4-inch-diameter holes were located near each end of the Class AA concrete, along with two 1-inch-diameter vent holes near the third points to help allow air to escape during the placement. In addition, two horizontal 1-1/2-inch-diameter holes were created as pick points to help maneuver the beams during fabrication. Details of the placement, vent, and access holes are shown in Figures 5.6 and 5.7.

Figure 5.7: Reinforcing Cages with PVC Inserts for Access Ports, Vent Holes, and Pick Points

Placement of the Class AA substrate portion for the FR-SCC repaired beam specimens involved first placing the reinforcing cages upside down within the formwork and securing the inserts, as shown in Figure 5.8(l). In addition, the portion of the stirrups within the subsequent repair zone were wrapped with black electrical tape in order to keep them clean and free from any contamination from the Class AA placement, as shown in Figure 5.6(r).

Figure 5.8: Upside Down Placement of Cages (l) and Protection of Exposed Portion of Stirrups (r)

The Class AA mix was delivered by Dolese Bros. and placed into the beam forms using a concrete bucket. The beams were filled in two layers. After the first layer was poured, the concrete was vibrated to reduce air pockets and ensure proper consolidation, as shown in Figure 5.9(l). The second layer was carefully placed and consolidated in order to leave the 6-inch-thick nominal FR-SCC repair zone along the top of the specimen. The concrete was carefully sloped to provide the subsequent FR-SCC repair a depth of 5 inches at one end and 7 inches at the other, as shown in Figure 5.9(r). Once the concrete started to initially stiffen, the edge of a trowel was used to roughen the surface to mimic the concrete removal process that would be used in the field for a repair of this type. The beams and companion small scale specimens were moist cured for 7 days.

Figure 5.9: Placement of Class AA Substrate for Full-Scale FR-SCC Repaired Beam Specimens

After 7 days of moist curing, the beams were removed from the forms and allowed to cure for the remaining 28 days within the Fears Structural Engineering Lab, as shown in Figure 5.10(l). The black electrical tape was removed from the exposed portions of the stirrups, and the PVC inserts for the access ports, vent holes, and pick points were also removed. The specimens then underwent hydro-demolition to remove the surface paste and any loose material in preparation for the repair material placement, as shown in Figure 5.10(r).

Figure 5.10: Preparation of Class AA Substrate for Full-Scale FR-SCC Repaired Beam Specimens

Preparation and placement of the FR-SCC repair material involved first rotating the Class AA portions of the beams right-side up and then installing the flexural reinforcement. The strain gage wires were fed through the vent holes, and the specimens were then placed into the formwork, as shown in Figure 5.11. The FR-SCC repair material was mixed within the 1-cubic-yard mixer housed within the Fears Structural Engineering Lab and placed with a concrete bucket and funnel through the 4-inch-diameter access port at one end of each specimen, as shown in Figure 5.12(l).

The specimens were then moist cured for 7 days, removed from the forms, and visually and acoustically inspected to insure complete coverage of the FR-SCC repair. A completed specimen is shown in Figure 5.12(r).

Figure 5.11: Preparation for FR-SCC Repair Material Placement

Figure 5.12: Placement of FR-SCC Repair Material (l) and Completed Specimen (r)

5.3 Testing of Full-Scale Beam Specimens

A schematic of the test setup is shown in Figure 5.13. This third point loading arrangement results in a constant moment region within the center third of the specimen. A photograph of a test specimen within the test fixture is shown in Figure 5.14. A 100-kip load cell was placed on top of the spreader beam to monitor the load being applied during the testing process. String pots were attached to metal angles adhered near midspan to monitor the beam's deflection. The load cell, two string pots, and two internal strain gages were connected to a data acquisition system to monitor the test during loading.

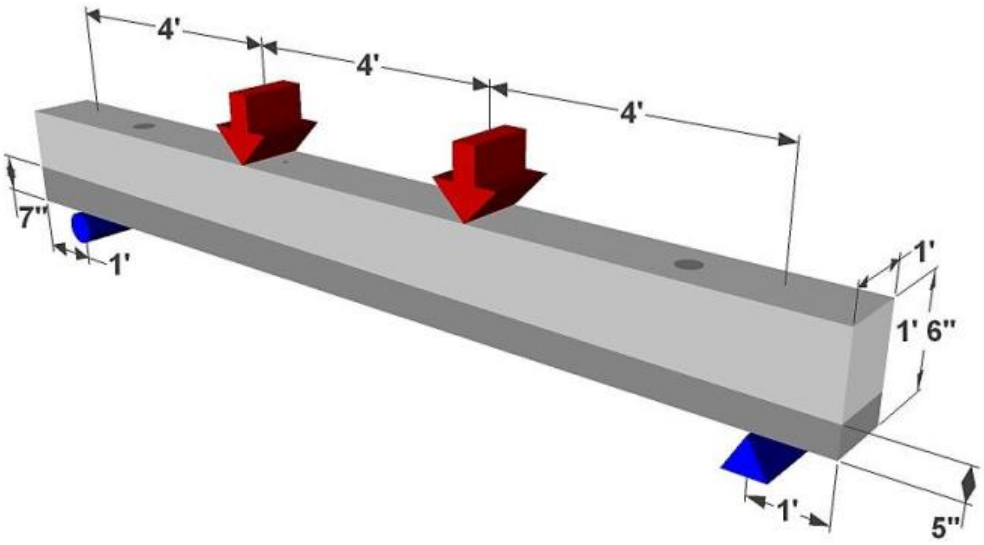

Figure 5.13: Schematic of Full-Scale Beam Specimen Test Setup

Figure 5.14: Photograph of Full-Scale Beam Specimen Test Setup

The specimen test procedure involved applying load in increments of 10 kips up to a total load of 80 kips. The load was then increased in increments of 5 kips until failure. After each load step, crack propagation patterns were traced, and the end of each crack was labeled with the current load amount. Failure was typically marked by an inability to sustain additional load on the specimen, or a crushing of the concrete within the center third of the beam along the top surface. In most cases, the specimen would continually deflect without taking additional load or failing completely, thereby arbitrary stopping points were established once the above failure conditions were met. At

this point, the data acquisition system was stopped, photographs were taken, and the beam was removed from the test setup.

A summary of the full-scale beam flexural test results is shown in Table 5.1, and the load-deflection plots of three representative specimens are shown in Figure 5.15. The nine specimens displayed very similar behavior except for slight differences in the cracking loads, with the FR-SCC exceeding the Class AA by 12% for the 10% Type K replacement material and 8% for the 15% Type K replacement material. Other than that slight difference, the peak loads and load-deflection responses were virtually identical. The first portion of the load-deflection response represents the behavior of the uncracked beams, which is primarily linear and depends on the uncracked section properties and moduli of elasticity of the specimens. The second portion, representing the post-cracking section up to flexural steel yielding, corresponds to the cracked beam with a reduced moment of inertia. The final portion, representing the steel yielding up to failure, corresponds to degradation of the stiffness of the beams as the degree of cracking intensifies and the steel continues to yield.

Table 5.1: Full-Scale Beam Specimen Test Results

Mix	Specimen	Cracking Load (kips)		Peak Load (kips)	
		Test Value	Average	Test Value	Average
Class AA	C-C-1	14.9	15.7	94.2	94.2
	C-C-2	16.4		93.9	
	C-C-3	15.8		94.6	
FR-SCC 10% Type K	C-10%-1	18.1	17.7	91.1	91.2
	C-10%-2	17.3		90.2	
	C-10%-3	17.7		92.3	
FR-SCC 15% Type K	C-15%-1	16.2	17.0	90.2	90.1
	C-15%-2	17.3		90.1	
	C-15%-3	17.5		90.1	

5.4 Evaluation of Full-Scale Beam Specimen Test Results

The results of the full-scale beam specimen testing indicate that the FR-SCC repair material restores the full flexural capacity of the repaired beams, with ultimate capacities virtually identical to the monolithic Class AA beam specimens. Furthermore, the synthetic fibers increased the cracking moment for the FR-SCC repaired beam specimens compared to the Class AA monolithic beams. The increase measured 12% for the 10% Type K replacement material and 8% for the 15% Type K replacement material. The overall load-deflection responses, shown in Figure 5.15, were also virtually identical between the FR-SCC repaired beam specimens and the Class AA monolithic beams.

In terms of the extent and morphology of the cracking behavior, all nine beams were very consistent, as shown in Figure 5.16. In general, the flexure and flexure-shear cracks of the repaired beams ran directly through the interface between the two materials (delineated with the red line in the photos), indicating that the beams were behaving monolithically. There were a few instances, however, where the cracks traversed horizontally a short distance along the interface before resuming their upward trend.

Based on the positive results of the full-scale beam flexural testing as well as those from the other evaluative tests of the FR-SCC repair material, the next step was to implement the FR-SCC repair material in the repair of an in-service bridge structure.

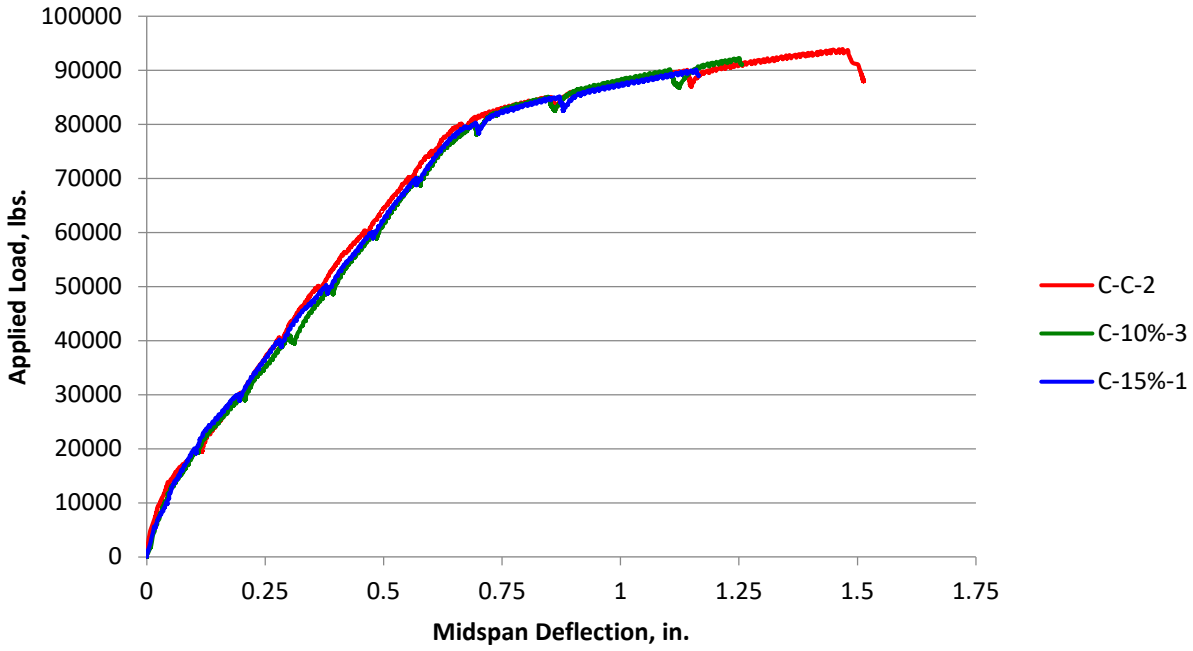

Figure 5.15: Full-Scale Beam Specimen Representative Load-Deflection Plots

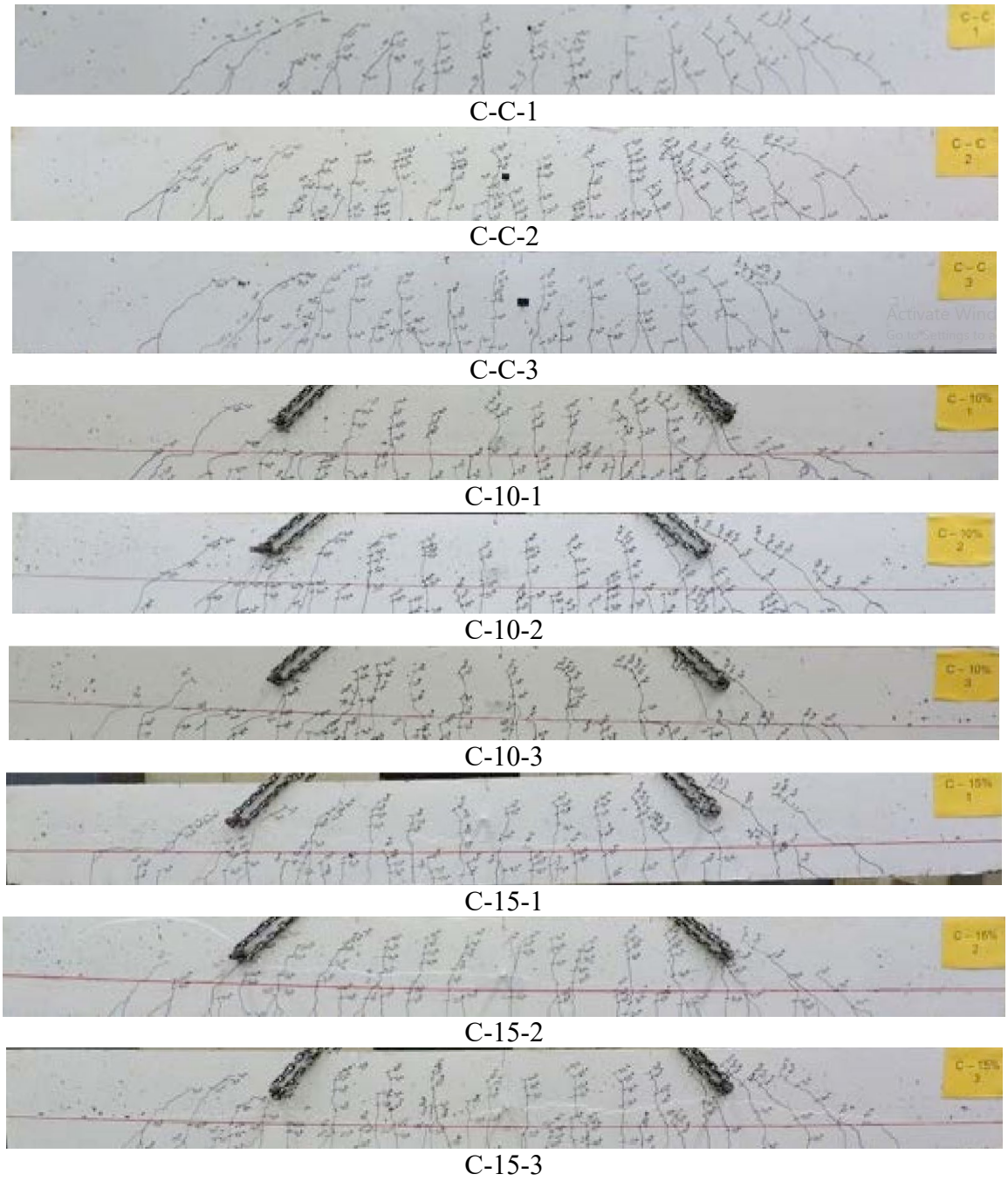

C-C-1

C-C-2

C-C-3

C-10-1

C-10-2

C-10-3

C-15-1

C-15-2

C-15-3

Figure 5.16: Specimen Crack Propagation During Flexural Testing

6 FIELD IMPLEMENTATION AND TESTING OF FULL-SCALE AASHTO TYPE II GIRDERS

The following chapter discusses the field implementation and subsequent testing of two full-scale AASHTO Type II prestressed girders. Based on the work described in the preceding chapters, the research team developed repair specifications and drawings for the I-244 Bridge Repair Project. These construction documents specified methods and extent of concrete removal, source material, submittals, trial batches, mock-ups, placement techniques, and testing of repaired areas. In addition, two girders were later identified for removal and subsequent testing in the lab – a control girder with no visible signs of deterioration and a significantly repaired girder using the FR-SCC repair material.

The I-244 Bridge over the Arkansas River was constructed in 1967 with a total length of almost 3,000 feet, and recent ODOT evaluations had classified the bridge structure as functionally obsolete, with an operating rating of 57.9 tons and an inventory rating of 35.0 tons. This bridge was particularly beneficial for two reasons. First, the bridge had undergone concrete repairs in the past that had performed poorly. Successful application of the FR-SCC would help convince ODOT of the value of this material for repairs to infrastructure throughout the State of Oklahoma. Second, the bridge was scheduled to be replaced. As such, the research team had the opportunity to repair an AASHTO Type II prestressed girder in service, after which it was removed and transported to the Fears Structural Engineering Lab at OU for testing. As a comparison, the research team also identified one identical girder for testing that had experienced minimal deterioration. This second girder served as a control to compare with the performance of the repaired girder. Photographs of the existing bridge are shown in Figures 6.1 and 6.2. Figure 6.2 highlights the previous concrete repairs.

Figure 6.1: Overall Views of the I-244 Bridge Over the Arkansas River

6.1 Testing of Full-Scale AASHTO Type II Control Girder

Based on a survey of the bridge superstructure, the research team identified one of the AASHTO Type II girders that would serve as the control girder for the comparative testing. This control girder had experienced minimal deterioration and was identical in design and construction to the

FR-SCC repaired girder. Figure 6.3(l) is a photograph of the span from which the control girder was removed, and Figure 6.3(r) is a photograph of the girder during delivery to Fears Lab by the repair contractor.

Figure 6.2: Previous Concrete Repairs to the I-244 Bridge Over the Arkansas River

Figure 6.3: Control Girder Span Location on Bridge (l) and Delivery to Structures Lab (r)

The full-scale AASHTO Type II control girder measured 46 feet in overall length with an 8-1/2-inch-thick deck. The bridge deck consisted of a 6-1/2-inch thick main slab portion with a 2-inch-thick wearing surface. However, due to difficulties involved in removing the girder from the bridge, the deck portion was not symmetrical with the girder. As a result, a supplemental 10-inch-wide portion of the deck was constructed in the lab to provide an overall symmetrical test specimen, as shown in Figure 6.4. Also shown in Figure 6.4 are the specimen dimensions and main reinforcement.

The test setup and protocol was selected to maximize the number of tests and to coincide with the most heavily repaired sections of the AASHTO Type II repaired girder, which were primarily located toward the ends of the girder span length. Deterioration of girder end regions is a typical

problem with prestressed concrete bridges due to leaking deck joints located at the supporting piers. The support and loading arrangements for the AASHTO girder tests are shown in Figures 6.5 and 6.6. Photographs of the test setup and instrumentation are shown in Figures 6.7 and 6.8, respectively.

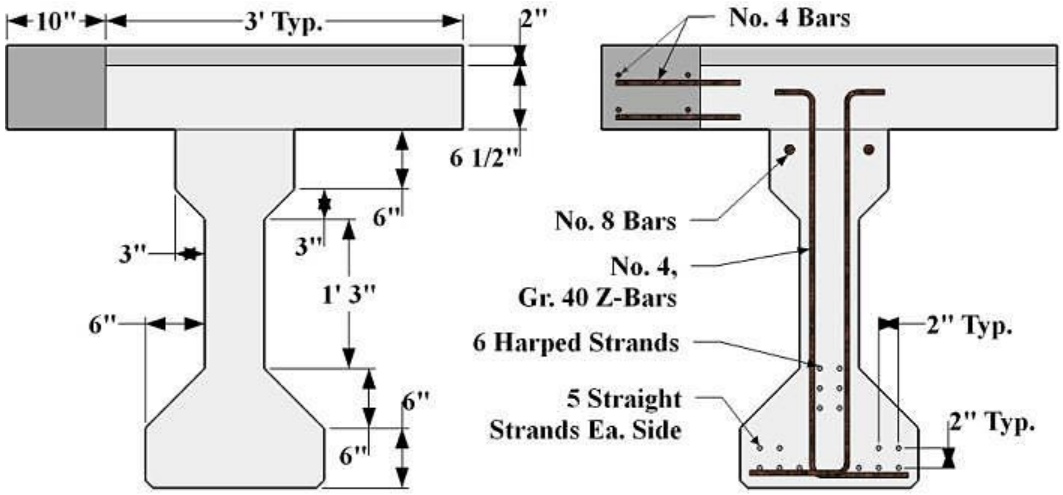

Figure 6.4: AASHTO Type II Girder Dimensions, Main Reinforcement, and Supplemental Deck

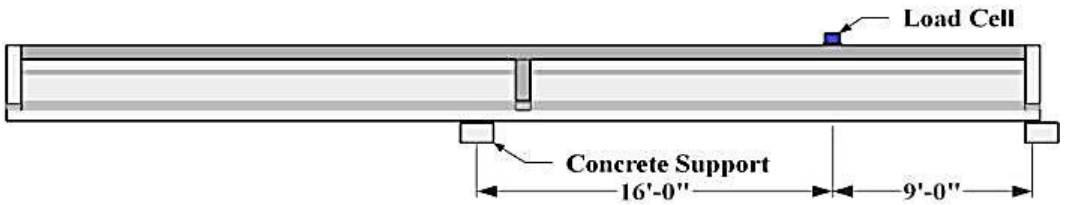

Figure 6.5: Test C1 Support Conditions (West Elevation)

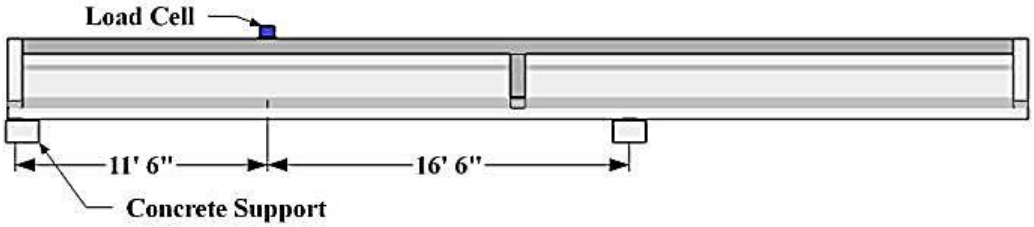

Figure 6.6: Test C2 Support Conditions (West Elevation)

Figure 6.7: AASHTO Girder C1 Test Setup

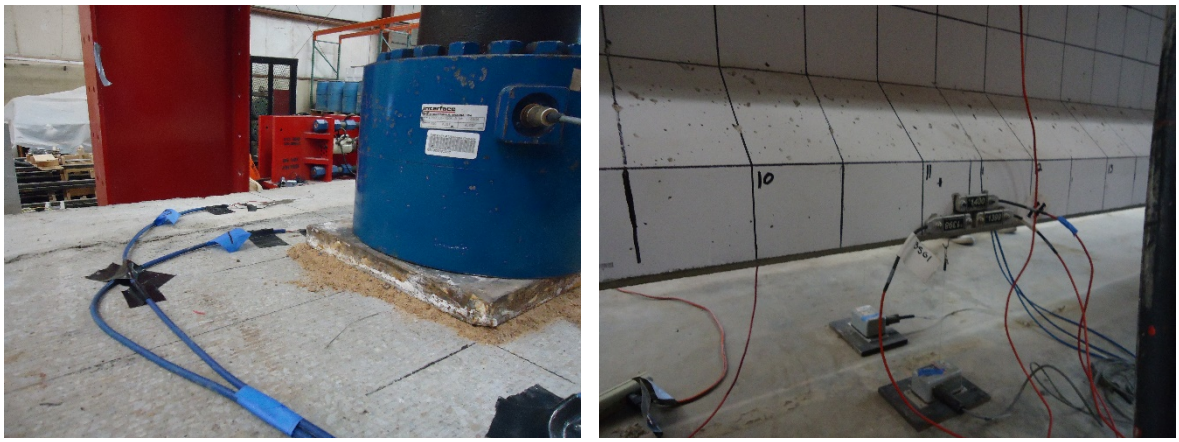

Figure 6.8: AASHTO Girder Instrumentation, Load Cell (l) and Wire Pots (r)

Testing of the AASHTO Type II control girder was completed for both the C1 and C2 support conditions. The load-deflection plots are shown in Figures 6.9 and 6.10, respectively. The failure mechanism for the C1 support condition test was identified as bond-shear failure, which is characterized by shear cracks migrating downward toward the strand, followed by splitting along the strand and finally slippage of the strand. Visible corrosion of the strands near the end of the girder likely contributed to the splitting-bond failure of the prestressing strands. The failure mechanism for the C2 support condition was identified as compression-shear failure, which is characterized by several shear cracks migrating upward toward the top of the girder, followed by a compression failure of the girder compression zone.

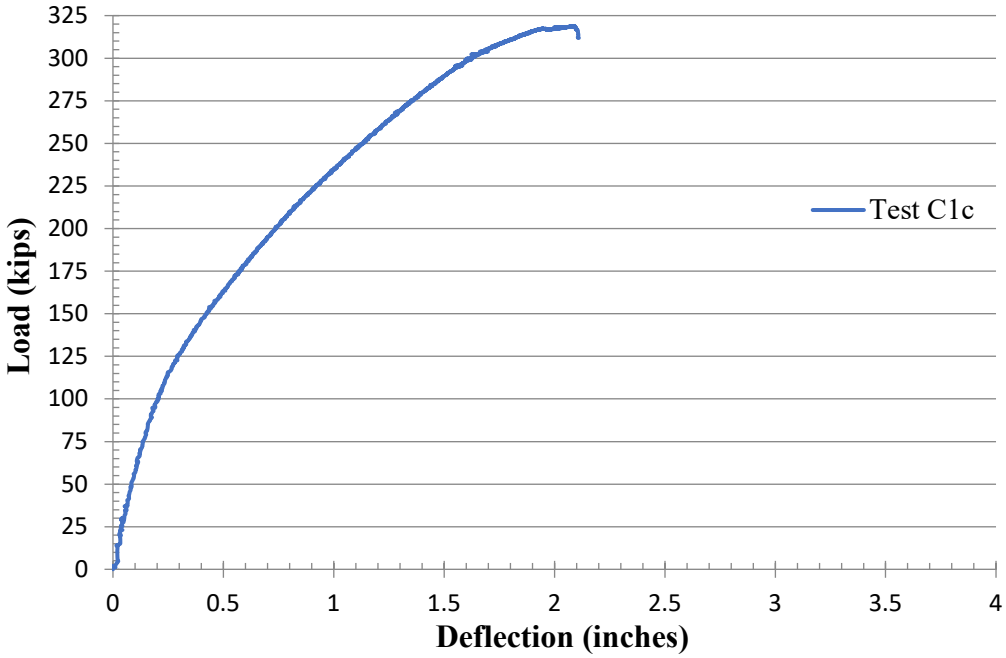

Figure 6.9: Control Girder C1 Support Condition Test (South End)

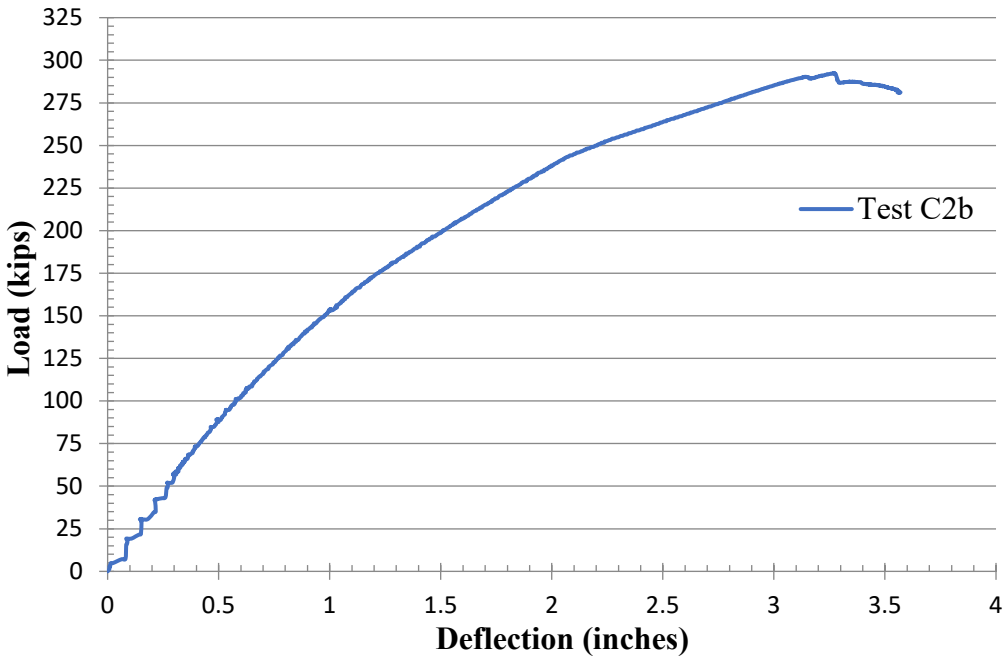

Figure 6.10: Control Girder C2 Support Condition Test (North End)

6.2 Testing of Full-Scale AASHTO Type II Repaired Girder

As mentioned previously, the FR-SCC repaired AASHTO Type II girder had extensive deterioration near the ends of the span, primarily as a result of leaking deck joints above the pier supports. The support conditions for the AASHTO Type II repaired girder were identical to the control girder and are shown in Figures 6.11 and 6.12. The red outlined portions represent the FR-SCC repaired areas of the girder, which are shown in photographs for the two end regions in Figures 6.13 and 6.14.

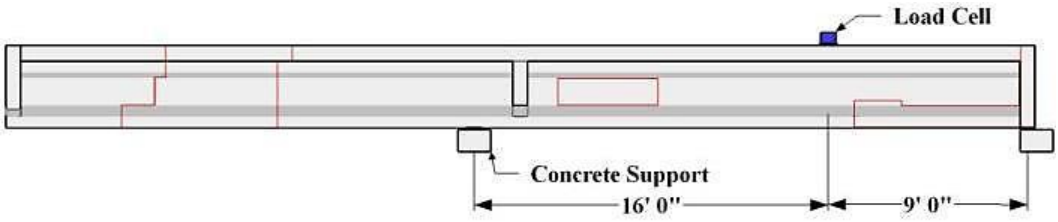

Figure 6.11: Test C1 Support Conditions (West Elevation)

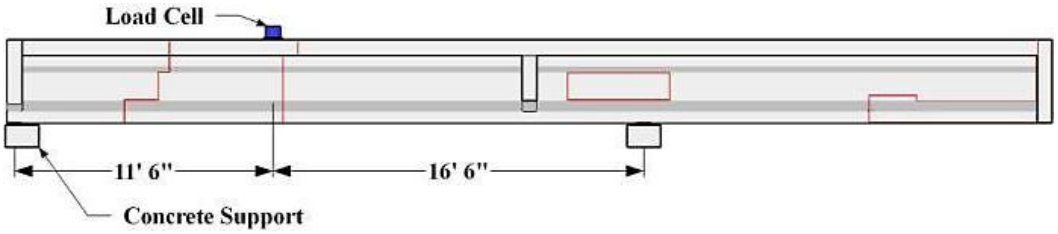

Figure 6.12: Test C2 Support Conditions (West Elevation)

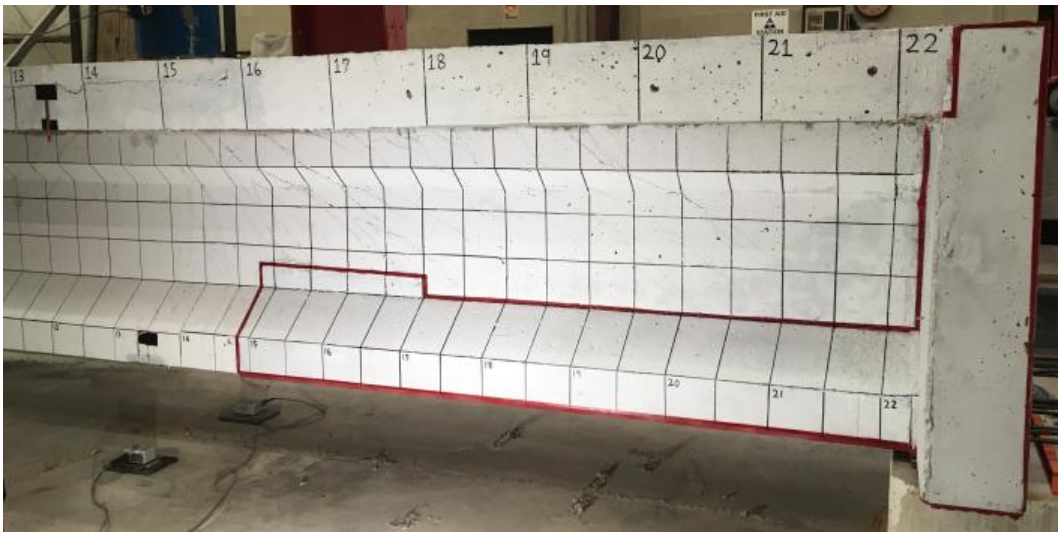

Figure 6.13: Photograph of Girder South End FR-SCC Repaired Region

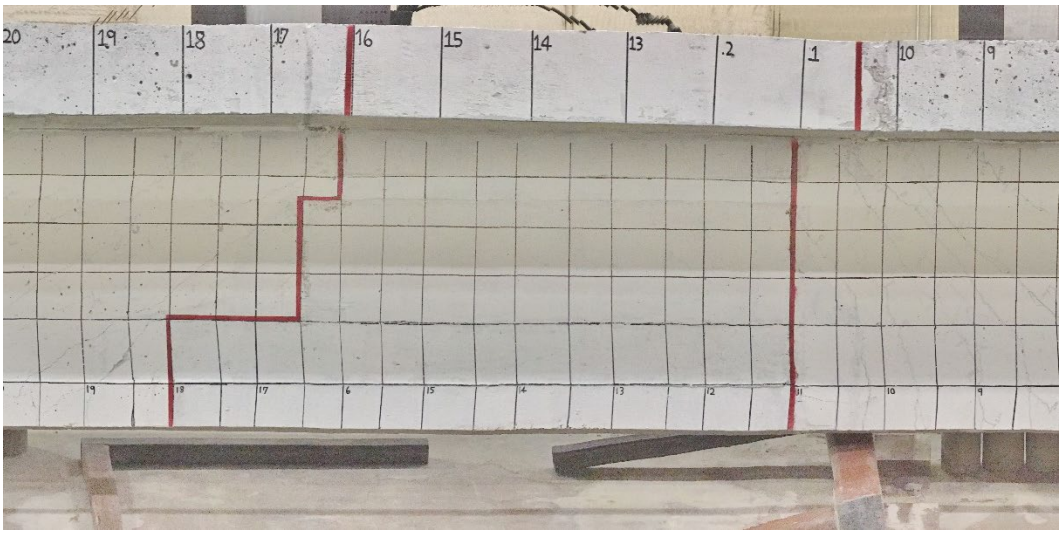

Figure 6.14: Photograph of Girder North End FR-SCC Repaired Region

Testing of the AASHTO Type II repaired girder was completed for both the C1 and C2 support conditions. The load-deflection plots are shown in Figures 6.15 and 6.16, respectively. The failure mechanism for the C1 support condition test was identified as bond slip of the prestressing strand. This may have been due corrosion of the strand within the end region even with the FR-SCC repair. As shown in Figure 6.17, the shear cracks extended continuously from the original concrete through the FR-SCC repaired region, indicating that the repair bonded well and acted monolithically with the original concrete.

The failure mechanism for the C2 support condition was identified as bond-shear failure, which is characterized by shear cracks migrating downward toward the strand, followed by splitting along the strand and finally slippage of the strand. As shown in Figure 6.18, the repair underwent extensive shear cracking, and the shear cracks extended continuously from the original concrete through the FR-SCC repaired region, indicating that the repair performed very well and also bonded well and acted monolithically with the original concrete.

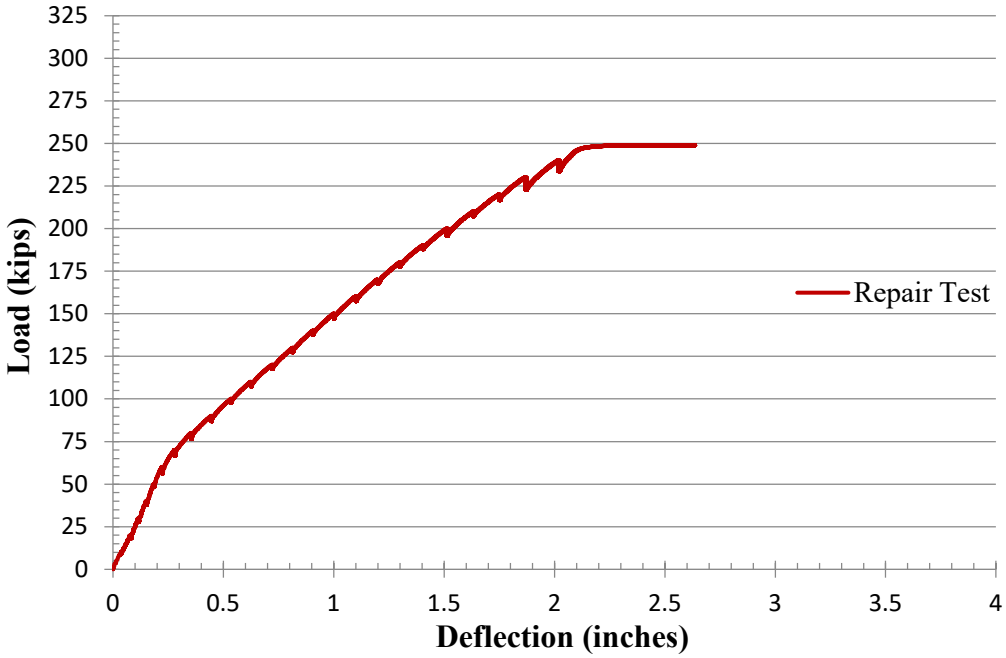

Figure 6.15: Repaired Girder C1 Support Condition Test (South End)

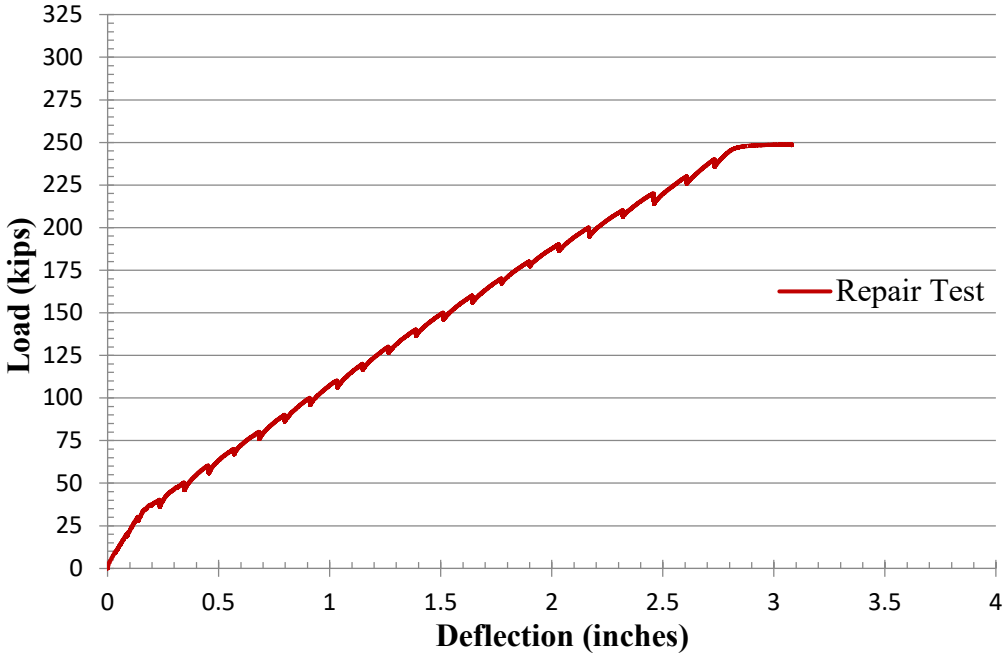

Figure 6.16: Repaired Girder C2 Support Condition Test (North End)

Figure 6.17: South End Region Repair at End of C1 Support Condition Testing

Figure 6.18: North End Region Repair at End of C2 Support Condition Testing

6.3 Comparison of Full-Scale AASHTO Type II Control and Repaired Girders

Figures 6.19 and 6.20 compare the load-deflection curves for the AASHTO Type II control and repaired girders. In general, the control girders were stiffer and experienced higher failure loads, with the repaired girder reaching 78% of the control girder capacity for the C1 support condition test and 85% of the control girder capacity for the C2 support condition test. However, the repaired girder did restore the necessary design capacity for the bridge, which is noticeable given the severe deterioration and reduced operating and inventory ratings for the bridge. As a result, the FR-SCC repair material is a viable repair option for bridges suffering severe deterioration.

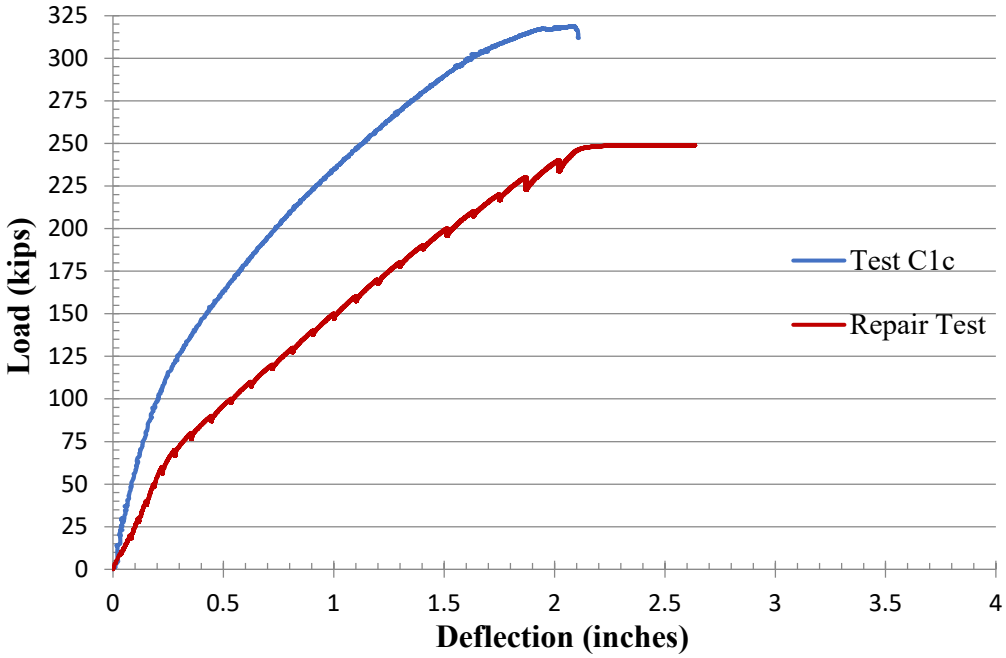

Figure 6.19: C1 Support Condition Test Comparison (South End)

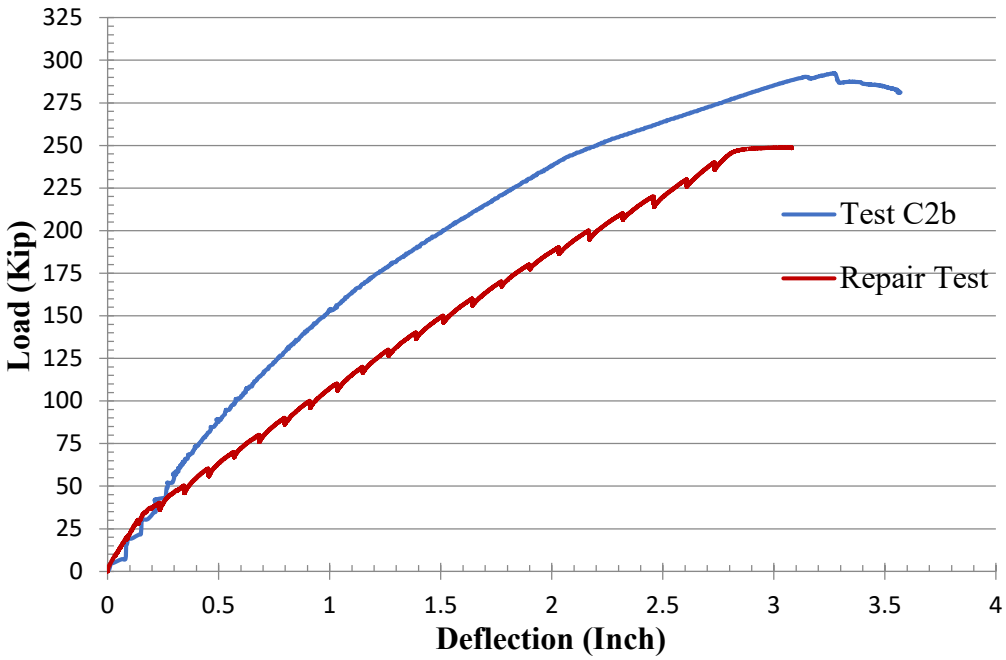

Figure 6.20: C2 Support Condition Test Comparison (North End)

REFERENCES

ACI 318-14. *Building Code Requirements for Structural Concrete (ACI 318-14)*. American Concrete Institute, Farmington Hills, MI, 2014.

Kassimi, Fodhil, El-Sayed, Ahmend K., Khayat, Kamal. "Performance of Fiber-Reinforced Self-Consolidating Concrete for Repair of Reinforced Concrete Beams." *ACI Structural Journal*. 2014. pp. 1277-1286.

Khayat, K.H., Hwang, S.-D., and Bonneau, O., Durability of SCC Used in Repair Applications, Presentation, ACI Spring Convention 2010.

Khayat, K.H., Petrov, N., Assaad, J., Morin, R., Thibault, M., "Performance of SCC Used in Repair of Retaining Wall Elements," Proc., 2nd North American Conf. on the Design and Use of Self-Consolidating Concrete, Ed. Shah, S., Chicago, Nov. 2005, 9 p.

Ozyildirim, C., "Use of SCC for the Repair of Bridge Substructures," Presentation, ACI Spring Convention 2013.

USDOT. "Deficient Bridges by State and Highway System 2013, Bridges and Structures." U.S. Department of Transportation Federal Highway Administration. <www.fhwa.dot.gov/bridge>.